

Electronic Supplementary Information for “Molecular dynamics Simulation of the Coalescence of Surfactant-Laden Droplets”

Soheil Arbabi,¹ Piotr Deuar,¹ Mateusz Denys,¹ Rachid
Bennacer,² Zhizhao Che,³ and Panagiotis E. Theodorakis^{1,*}

¹*Institute of Physics, Polish Academy of Sciences,
Al. Lotników 32/46, 02-668 Warsaw, Poland*

²*Université Paris-Saclay, CentraleSupélec, ENS Paris-Saclay, CNRS,
LMPS - Laboratoire de Mécanique Paris-Saclay, 91190, Gif-sur-Yvette, France*

³*State Key Laboratory of Engines, Tianjin University, 300350 Tianjin, China*

(Dated: September 27, 2023)

CONTENTS

MASS TRANSPORT MECHANISM	1
BRIDGE GROWTH DYNAMICS	13
WATER FLOW VELOCITY	16
VELOCITY OF APPROACH	17
ASPHERICITY OF THE DROPLETS	19
MOVIES	21
REFERENCES	22

MASS TRANSPORT MECHANISM

Figures S1, S2, and S3 illustrate droplet snapshots for different concentrations in the power-law regime for droplets with C10E4, C10E8, and Silwet-L77 surfactant, respectively,

* panos@ifpan.edu.pl

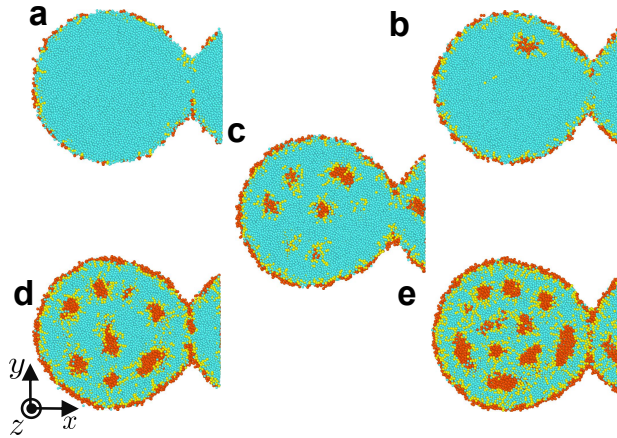


FIG. S1. Droplet interiors in the inertial regime showing the presence of new aggregates emerging during the coalescence process. Cross-sections are shown at times roughly corresponding to Fig. 1c by bridge radius for C10E4 in different concentrations, as follows: (a) 6.2 wt%, $t_c + 45.00 \tau$; (b) 12.3 wt%, $t_c + 47.50 \tau$; (c) 24.2 wt%, $t_c + 48.75 \tau$; (d) 35.4 wt%, $t_c + 63.75 \tau$ (e) 46.2 wt%, $t_c + 92.5 \tau$.

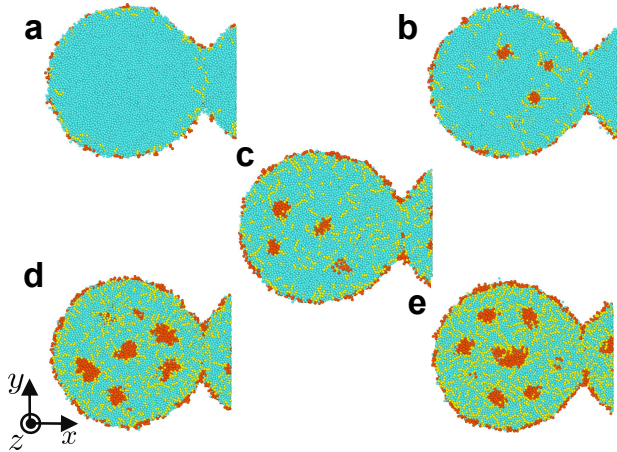


FIG. S2. Droplet interiors in the inertial regime showing the presence of new aggregates emerging during the coalescence process. Cross-sections are shown at times roughly corresponding to Fig. 1c by bridge radius for C10E8 in different concentrations, as follows: (a) 6.2 wt%, $t_c + 50.00 \tau$; (b) 12.3 wt%, $t_c + 52.50 \tau$; (c) 24.2 wt%, $t_c + 70.00 \tau$; (d) 35.4 wt%, $t_c + 85.00 \tau$; (e) 46.2 wt%, $t_c + 92.50 \tau$.

which complement our data in Fig. 6 of the manuscript.

The information provided in Tables S1, S2, and S3 reveals that while a significant proportion of molecules from the surface of the droplets in the contact area are transported to the surface of the resulting bridge during coalescence, some of these molecules become trapped and remain within the bulk of the formed droplet (as evidenced by the increased count in the bulk).

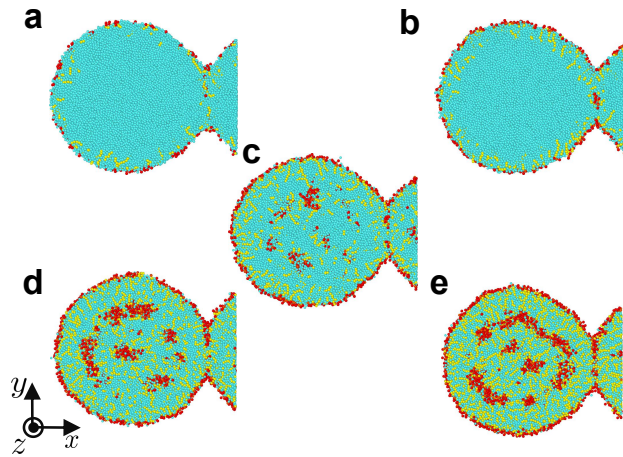


FIG. S3. Droplet interiors in the inertial regime showing the presence of new aggregates emerging during the coalescence process. Cross-sections are shown at times roughly corresponding to Fig. 1c by bridge radius for Silwet-L77 in different concentrations, as follow: (a) 7.6 wt%, $t_c + 32.50 \tau$; (b) 14.8 wt%, $t_c + 53.75 \tau$; (c) 28.2 wt%, $t_c + 68.75 \tau$; (d) 40.3 wt%, $t_c + 81.25 \tau$; (e) 51.2 wt%, $t_c + 93.75 \tau$.

The relative contributions from surfactant transport processes from one part of a droplet to others over short time scales $\Delta t'$ are reported in Table S4 for three types of surfactant and the range of concentrations considered in our study. Fig. S4 shows cross-sections of the evolving droplets for C10E4, complementing also Fig. 6 of the manuscript.

TABLE S1. Number of surfactant molecules (C10E4) before pinching (“Initial snapshot”, for example, see Fig. 1a) and at the end (“Last snapshot”, for example, see Fig. 1e) of the coalescence process in the bulk and at the surface of the droplets.

Concentration (wt%):	6.25	12.37	24.18	35.48	46.09
Initial snapshot (two droplets)					
Bulk	0	202	2184	4096	5899
Surface	1428	2656	3530	4476	5529
Last snapshot (one droplet)					
Bulk	10	234	2229	4329	6167
Surface	1418	2624	3485	4243	5261

TABLE S2. Number of surfactant molecules (C10E8) before pinching (“Initial snapshot”, for example see Fig. 1a) and at the end (“Last snapshot”, for example, see Fig. 1e) of the coalescence process in the bulk and at the surface of the droplets.

Concentration (wt%):	6.25	12.37	24.18	35.48	46.09
Initial snapshot (two droplets)					
Bulk	0	379	1429	2514	3579
Surface	910	1439	2207	2940	3693
Last snapshot (one droplet)					
Bulk	11	400	1511	2603	3782
Surface	899	1418	2125	2851	3490

TABLE S3. Number of surfactant molecules (Silwet-L77) before pinching (“Initial snapshot”, for example see Fig. 1a) and at the end (“Last snapshot”, for example, see Fig. 1e) of the coalescence process in the bulk and at the surface of the droplets.

Concentration (wt%):	7.6	14.8	28.2	40.3	51.2
Initial snapshot (two droplets)					
Bulk	0	8	939	2056	3122
Surface	910	1810	2697	3398	4150
Last snapshot (one droplet)					
Bulk	15	27	997	2221	3374
Surface	895	1791	2639	3233	3898

TABLE S4: Summary of the relative contributions from all relevant surfactant transport processes in the coalescing droplets. The table lists the relative frequency of transport from one region to another over a time interval $\Delta t' = 1.25\tau$ as a percentage of the mean number of surfactant molecules in source regions. Data was averaged over consecutive snapshots made at $\Delta t'$ intervals during the entire coalescence process which lasts $\mathcal{O}(1000 - 2000)\tau$. CAC ≈ 7.5 wt% for C10E4 and C10E8.

Probabilities						
Concentration (wt%)	C10E4 and C10E8					
	6.25	12.37	24.18	35.48	46.09	
Silwet-L77						
	7.61	14.82	28.21	40.25	51.19	
Remaining at bridge bulk						
C10E4	0.8774	0.8098	0.8765	0.8647	0.8529	
C10E8	0.8728	0.8435	0.8693	0.8669	0.8741	
Silwet-L77	0.8915	0.8904	0.8814	0.8192	0.7958	
Movement from bridge bulk to left surface						
C10E4	0.0000	0.0000	0.0005	0.0003	0.0004	
C10E8	0.0000	0.0000	0.0001	0.0002	0.0004	
Silwet-L77	0.0000	0.0015	9.1e-5	0.0002	0.0005	
Movement from bridge bulk to left bulk						
C10E4	0.0066	0.0093	0.0648	0.0388	0.0388	
C10E8	0.0075	0.0472	0.0460	0.0419	0.0403	
Silwet-L77	0.0052	0.0068	0.0337	0.0392	0.0403	
Movement from bridge bulk to bridge surface						
C10E4	0.1092	0.1542	0.0326	0.0575	0.0685	
C10E8	0.1081	0.0642	0.0424	0.0504	0.0428	
Silwet-L77	0.0912	0.0882	0.05551	0.1017	0.1254	
Movement from bridge bulk to right surface						
C10E4	0.0000	0.0008	9.7e-5	0.0004	0.0004	
C10E8	0.0000	0.0004	0.0004	9.7e-5	0.0007	
Silwet-L77	0.0000	0.0000	9.1e-5	0.0002	0.0008	

Cont. next page...

Concentration (wt%)	C10E4 and C10E8				
	6.25	12.37	24.18	35.48	46.09
Silwet-L77					
	7.61	14.82	28.21	40.25	51.19
Movement from bridge bulk to right bulk					
C10E4	0.0066	0.0257	0.0252	0.0381	0.0388
C10E8	0.0113	0.0444	0.0413	0.0402	0.0413
Silwet-L77	0.0119	0.0129	0.0290	0.0391	0.0370
Remaining at bridge surface					
C10E4	0.9398	0.9284	0.9360	0.9244	0.9099
C10E8	0.9284	0.9428	0.9352	0.9249	0.9251
Silwet-L77	0.9307	0.9494	0.9375	0.9083	0.9065
Movement from bridge surface to left surface					
C10E4	0.0275	0.0305	0.0260	0.0237	0.0259
C10E8	0.0330	0.0256	0.0258	0.0278	0.0253
Silwet-L77	0.0315	0.0227	0.0251	0.02893	0.0254
Movement from bridge surface to left bulk					
C10E4	0.0001	0.0001	5.5e-5	0.0001	0.0003
C10E8	0.0000	0.000	0.0001	0.0002	0.0003
Silwet-L77	9.4e-5	0.0000	3.4e-5	0.0001	0.0002
Movement from bridge surface to bridge bulk					
C10E4	0.0042	0.0103	0.0098	0.0262	0.0373
C10E8	0.0057	0.0087	0.0129	0.0181	0.0235
Silwet-L77	0.0077	0.0045	0.0110	0.0321	0.0417
Movement from bridge surface to right surface					
C10E4	0.0281	0.0304	0.0279	0.0251	0.0261
C10E8	0.0326	0.0226	0.0255	0.0284	0.0252
Silwet-L77	0.0298	0.02317	0.0260	0.0300	0.0257

Cont. next page...

Concentration (wt%)	C10E4 and C10E8				
	6.25	12.37	24.18	35.48	46.09
Silwet-L77					
	7.61	14.82	28.21	40.25	51.19
Movement from bridge surface to right bulk					
C10E4	0.0000	2.5e-5	4.1e-5	0.0003	0.0002
C10E8	8.7e-5	5.8e-5	0.0001	0.0002	0.0004
Silwet-L77	0.0000	0.0000	3.4e-5	0.0002	0.0002
Remaining at left bulk					
C10E4	0.9332	0.9849	0.9894	0.9877	0.9835
C10E8	0.9074	0.9945	0.9870	0.9864	0.9803
Silwet-L77	0.9171	0.9210	0.9934	0.9913	0.9825
Movement from left bulk to left surface					
C10E4	0.0046	0.0092	0.0052	0.0092	0.0138
C10E8	0.0092	0.0012	0.0095	0.0111	0.0158
Silwet-L77	0.0213	0.0396	0.0027	0.0055	0.0150
Movement from left bulk to bulk bridge					
C10E4	0.0000	0.00021	0.0031	0.0012	0.0011
C10E8	0.0000	0.0019	0.0021	0.0008	0.0010
Silwet-L77	0.0000	0.0015	0.0009	0.0010	0.0011
Movement from left bulk to surface bridge					
C10E4	0.0000	0.0000	9.7e-6	4.9e-6	1.1e-5
C10E8	0.0000	0.0000	1.9e-5	9.8e-6	1.8e-5
Silwet-L77	0.0000	0.0000	0.00000	6.8e-6	1.3e-5
Movement from left bulk to right surface					
C10E4	0.0000	0.0003	2.4e-5	3.5e-5	6.2e-5
C10E8	0.0000	0.0002	2.4e-5	2.7e-5	2.7e-5
Silwet-L77	0.0000	0.0024	3.2e-5	5.2e-5	6.7e-5

Cont. next page...

Concentration (wt%)	C10E4 and C10E8				
	6.25	12.37	24.18	35.48	46.09
Silwet-L77					
	7.61	14.82	28.21	40.25	51.19
Movement from left bulk to right bulk					
C10E4	0.0621	0.0052	0.0020	0.0018	0.0013
C10E8	0.0833	0.0020	0.0011	0.0015	0.0026
Silwet-L77	0.0615	0.035	0.0027	0.0020	0.0011
Remaining at left surface					
C10E4	0.9942	0.9922	0.9912	0.9863	0.9801
C10E8	0.9931	0.9948	0.9887	0.9859	0.9788
Silwet-L77	0.9947	0.9956	0.9954	0.9926	0.9840
Movement from left surface to left bulk					
C10E4	2.1e-5	0.0008	0.0034	0.0094	0.0159
C10E8	5.9e-5	0.0003	0.0067	0.0104	0.0168
Silwet-L77	0.0001	0.0004	0.0010	0.0037	0.0126
Movement from left surface to bridge bulk					
C10E4	0.0000	0.0000	1.6e-5	5.8e-6	1.4e-5
C10E8	1.2e-5	0.0000	3.4e-6	9.1e-7	1.7e-5
Silwet-L77	0.0000	0.0000	0.0000	5.7e-7	7.6e-6
Movement from left surface to bridge surface					
C10E4	0.0032	0.0037	0.0029	0.0017	0.0018
C10E8	0.0045	0.0027	0.0032	0.0015	0.0014
Silwet-L77	0.0033	0.0022	0.0015	0.0017	0.0019
Movement from left surface to right surface					
C10E4	0.0025	0.0031	0.0029	0.0024	0.0019
C10E8	0.0022	0.0020	0.0012	0.0020	0.0028
Silwet-L77	0.0017	0.0015	0.0019	0.0017	0.0012

Cont. next page...

Concentration (wt%)	C10E4 and C10E8				
	6.25	12.37	24.18	35.48	46.09
Silwet-L77					
	7.61	14.82	28.21	40.25	51.19
Movement from left surface to right bulk					
C10E4	0.0000	2.8e-5	1.1e-5	3.2e-5	6.5e-5
C10E8	1.2e-5	3.0e-5	2.4e-5	3.1e-5	1.7e-5
Silwet-L77	0.0000	2.0e-5	1.0e-5	3.4e-5	5.2e-5
Remaining at right bulk					
C10E4	0.9251	0.9831	0.9900	0.9875	0.9831
C10E8	0.9103	0.9926	0.9871	0.9859	0.9808
Silwet-L77	0.9493	0.9155	0.9937	0.9912	0.9833
Movement from right bulk to right surface					
C10E4	0.0000	0.0096	0.0068	0.0094	0.0142
C10E8	0.0373	0.0033	0.0097	0.0116	0.0153
Silwet-L77	0.0059	0.0428	0.0025	0.0056	0.0143
Movement from right bulk to bulk bridge					
C10E4	0.0000	0.0018	0.0011	0.0011	0.0011
C10E8	0.0000	0.0018	0.0019	0.0007	0.0010
Silwet-L77	0.0000	0.0015	0.0008	0.0010	0.0010
Movement from right bulk to surface bridge					
C10E4	0.0000	0.0000	2.4e-6	1.1e-5	1.4e-5
C10E8	0.0000	0.0000	2.8e-5	7.9e-6	1.9e-5
Silwet-L77	0.0000	0.0000	2.7e-6	6.85e-6	2.0e-5
Movement from right bulk to left surface					
C10E4	0.0000	0.0001	1.9e-5	2.7e-5	5.0e-5
C10E8	0.0014	0.0001	1.9e-5	2.9e-5	2.7e-5
Silwet-L77	0.0000	0.0018	2.4e-5	5.4e-5	7.3e-5

Cont. next page...

Concentration (wt%)	C10E4 and C10E8				
	6.25	12.37	24.18	35.48	46.09
Silwet-L77					
	7.61	14.82	28.21	40.25	51.19
Movement from right bulk to left bulk					
C10E4	0.0748	0.0051	0.0019	0.0018	0.0013
C10E8	0.0508	0.0019	0.0011	0.0015	0.0026
Silwet-L77	0.0447	0.0381	0.002	0.0020	0.0011
Remaining at right surface					
C10E4	0.9940	0.9923	0.9898	0.9859	0.9795
C10E8	0.9932	0.9946	0.9884	0.9856	0.9793
Silwet-L77	0.9948	0.9956	0.9954	0.9926	0.9845
Movement from right surface to right bulk					
C10E4	0.0000	0.0008	0.0045	0.0096	0.0165
C10E8	0.0002	0.0010	0.0069	0.0107	0.0163
Silwet-L77	8.10e-5	0.0004	0.0009	0.0037	0.0121
Movement from right surface to bridge bulk					
C10E4	0.0000	0.0000	4.7e-6	9.9e-6	7.7e-6
C10E8	0.0000	0.0000	1.4e-5	3.6e-6	1.9e-5
Silwet-L77	0.0000	0.0000	1.0e-6	3.4e-6	1.3e-5
Movement from right surface to bridge surface					
C10E4	0.0033	0.0036	0.0031	0.0019	0.0018
C10E8	0.0043	0.0023	0.0032	0.0015	0.0013
Silwet-L77	0.0032	0.0022	0.0015	0.0018	0.0019
Movement from right surface to left surface					
C10E4	0.0025	0.0031	0.0024	0.0024	0.0019
C10E8	0.0021	0.0019	0.0013	0.0020	0.0028
Silwet-L77	0.0017	0.0016	0.0019	0.0016	0.0012

Cont. next page...

Concentration (wt%)	C10E4 and C10E8				
	6.25	12.37	24.18	35.48	46.09
Silwet-L77					
	7.61	14.82	28.21	40.25	51.19
Movement from right surface to left bulk					
C10E4	0.0000	2.2e-5	1.4e-5	3.3e-5	7.5e-5
C10E8	1.1e-5	3.6e-5	1.7e-5	2.5e-5	3.4e-5
Silwet-L77	0.0000	3.0e-5	9.2e-6	3.2e-5	4.9e-5

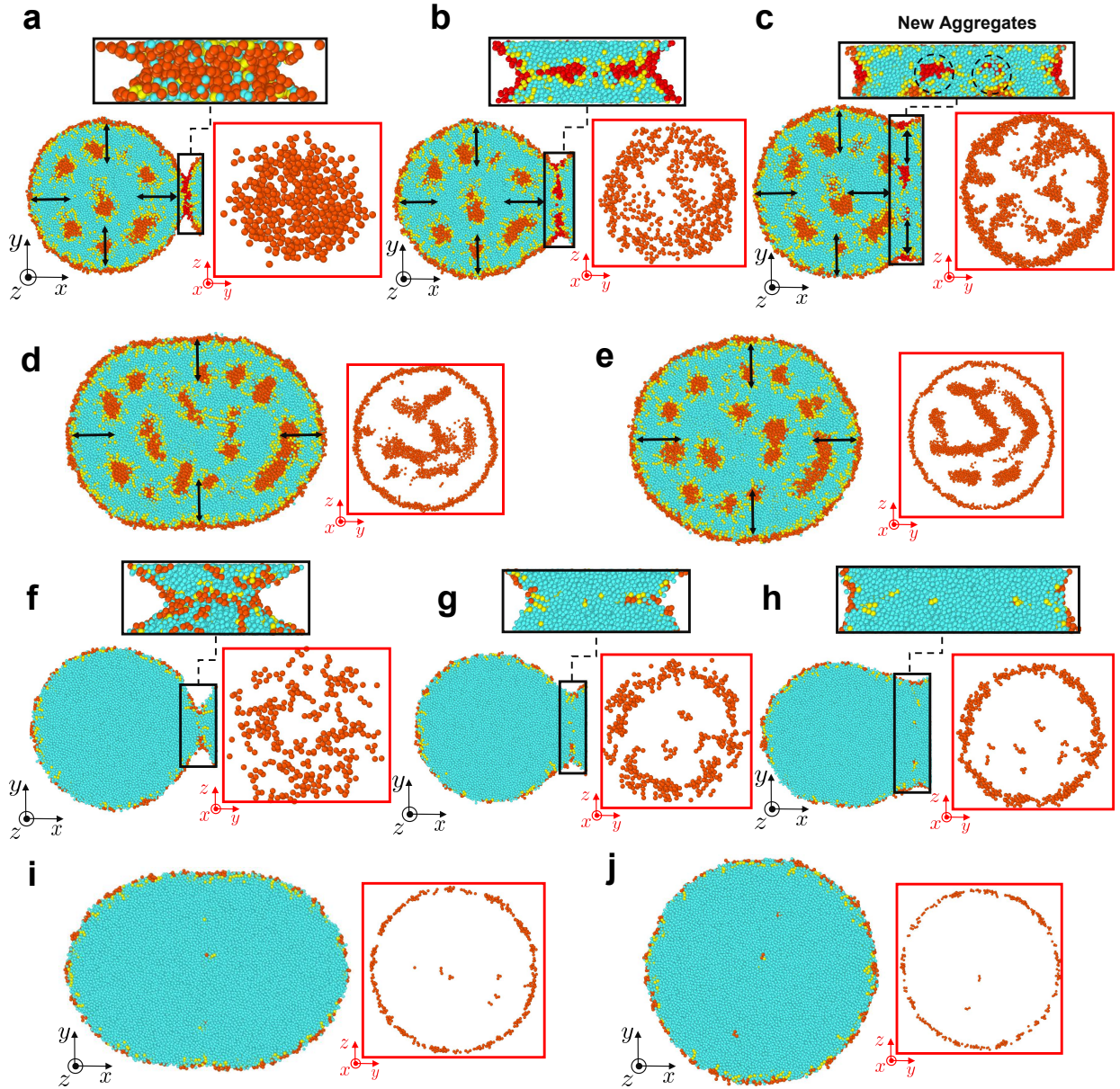


FIG. S4. Mass transport mechanism of surfactant (C10E4) during the coalescence process, for concentrations above (upper panels) and below (lower panels) CAC. The length of the arrows reflects the probabilities associated with surfactant transport to the different droplet areas as reported in Table S4. Above the CAC (a–e, 35.48 wt%) snapshots were obtained at times (a) $t_c + 32.5 \tau$, (b) $t_c + 76.25 \tau$, (c) $t_c + 233.75 \tau$, (d) $t_c + 517.50 \tau$, (e) $t_c + 1358.75 \tau$, while below the CAC (f–j, 6.25 wt%) times shown are (f) $t_c + 20 \tau$, (g) $t_c + 55 \tau$, (h) $t_c + 100 \tau$, (i) $t_c + 197.5 \tau$, (j) $t_c + 283.75 \tau$. Different stages of the coalescence process are shown: soon after the end of the thermal regime (a, f), the development of the bridge and the formation of new aggregates (b, g) or surfactant monomers remaining in the bridge region (c, h), and the full development of the bridge (d, i) towards the final equilibrium state (e, j). Magnified views of the bridge region and its cross-section (showing only surfactant hydrophobic beads in the bridge region, red) are shown above and to the right of the snapshots, respectively.

BRIDGE GROWTH DYNAMICS

The average velocity (b/t) of bridge growth is reported in Table S5. It shows that adding surfactant reduces the average velocity in all cases. However, we see interesting behaviour for Silwet-L77, which is the fastest among surfactant-laden droplets in the lowest concentration but in higher concentrations Silwet-L77 is the slowest one. This behaviour also is confirmed when we compare later the velocities of approach. In low concentrations (below CAC), Silwet-L77 makes less aggregates and they have low density, which helps the droplets to coalesce faster. However, when it comes to higher concentrations, Silwet-L77 aggregates are more in quantity and surface tension is the smallest in Silwet-L77. Both of these properties make coalescence slower in higher concentrations for Silwet-L77.

In Fig. S5, the bridge growth rate of pure water and in the highest concentration (46.2 wt%) of C10E4 are plotted. In both curves the values of the thermal length scale ($l_{\text{Thermal}} = (k_B T / \gamma)^{1/4} R_0^{1/2}$) [1] are marked using horizontal lines which is $l_w = 4.0 \sigma$ for pure water and $l_s = 5 \sigma$ for surfactant-laden droplets. It is seen that this is an excellent match to the early non-changing bridge radius. This crossover takes more time and is more pronounced in case of surfactant-laden drops, presumably due to the reduction of surface tension due to presence of surfactant. We also report on the bridge growth dynamics for all concentrations in the case of C10E8 (Fig. S6a) and Silwet-L77 (Fig. S6b), in complement to Fig. 9 of the main manuscript.

TABLE S5. Average velocity of bridge growth in units σ/τ from t_c until the full development of the bridge (for example, see snapshots of Fig. 1d of the main manuscript). ^a

Concentration (wt%)	C10E4 and C10E8				
	6.25	12.37	24.18	35.48	46.09
Silwet-L77			28.21	40.25	51.19
	7.61	14.82			
C10E4	0.2849	0.2204	0.1878	0.1605	0.1047
C10E8	0.2794	0.2319	0.1871	0.1530	0.1115
Silwet-L77	0.2912	0.2029	0.1550	0.1034	0.0655
CAC(C10E4 and C10E8) \simeq 7.5) wt%					
CAC(Silwet-L77) \simeq 16.23 wt%					

^a For pure water droplets in the viscous regime (result from simulation): 0.3675 σ/τ

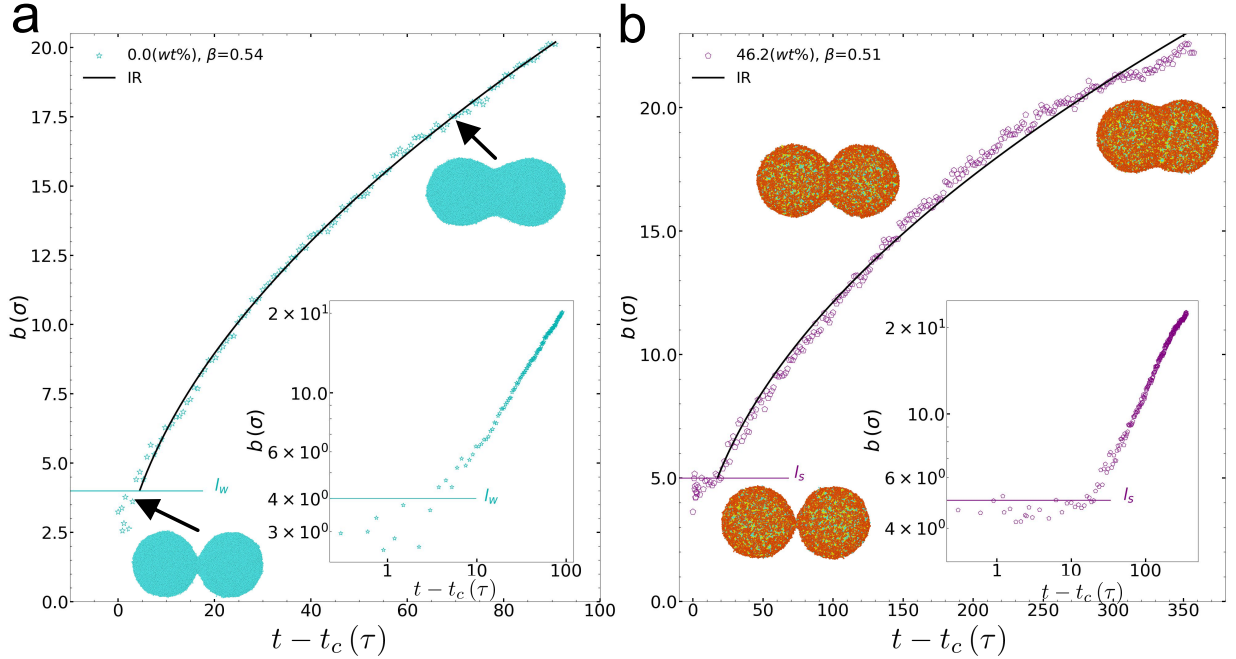


FIG. S5. a) Bridge growth rate in the case of pure water droplets. When the bridge radius, b , reaches the thermal length scale for pure water ($l_w = 4 \sigma$), hydrodynamics effect play the main role and a fast transition between thermal and inertial regimes occurs. b) Bridge growth rate of surfactant-laden droplets (C10E4, 46.2 wt%). When the bridge radius reaches the thermal length scale for surfactant-laden droplets ($l_s = 5 \sigma$), the transition occurs as well, but subsequent growth is slower than in pure water.

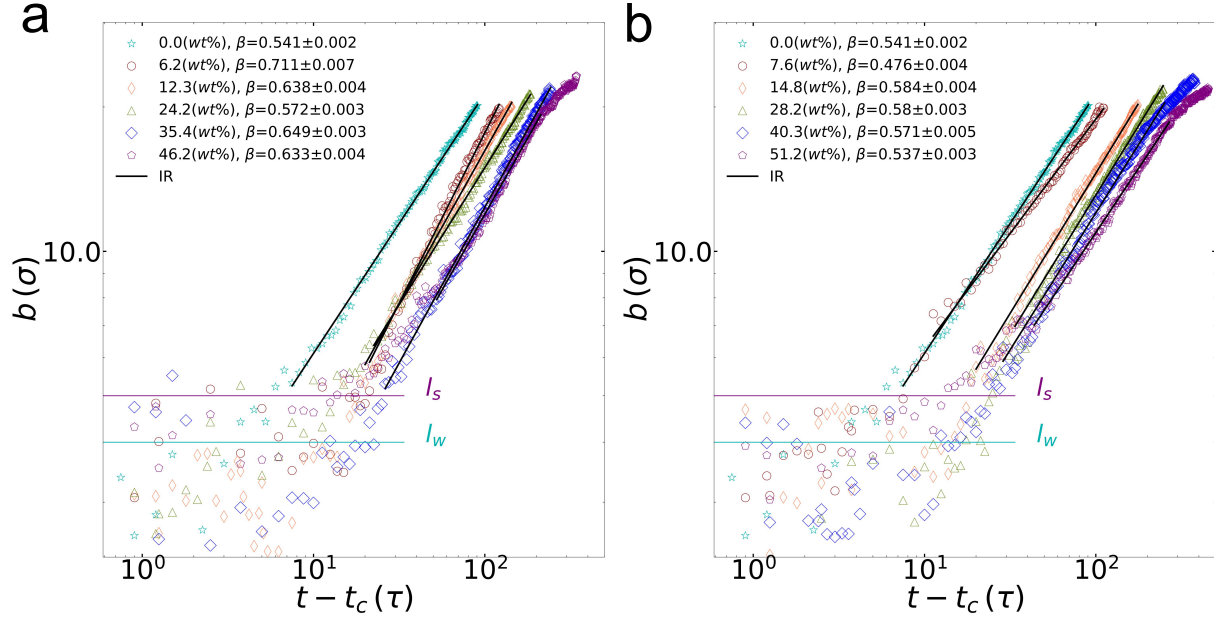


FIG. S6. Bridge growth rate in the case of a) C10E8 and b) Silwet-L77 for different concentrations in wt%, as indicated. Increasing the surfactant concentration makes the bridge growth slower and transition between thermal and inertial regime takes more time. Power-law fits $\sim t^\beta$ are shown, labeled ‘IR’. l_s is the thermal length in the case of surfactant-laden droplets above CAC, while l_w is the thermal length in the case of pure water droplets. Notation like in Fig. 9 of the main manuscript, with b being the bridge radius and t_c the time of the establishment of the permanent contact between the droplets.

WATER FLOW VELOCITY

TABLE S6. Average velocity of water flow in the direction, X , of the droplets approach for pure water droplets in units σ/τ . The velocities are separately averaged for inward and outward flowing grids (colors in Fig. 8 of the manuscript) to show the relative importance of the difference between inflow and outflow.

$t(\tau)$	$t_c + [0, 7.5]$	$t_c + [8.25, 27.75]$	$t_c + [28.5, 89.25]$
$b(\sigma)$	$3.2 < b < 5.4$	$5.58 < b < 10.90$	$11.00 < b < 20.11$
Toward bridge (System)	0.1946 ± 0.0016	0.1926 ± 0.0013	0.2001 ± 0.0008
Away from bridge (System)	0.1943 ± 0.0018	0.1808 ± 0.0019	0.1660 ± 0.0011
Toward centre (In bridge)	0.298 ± 0.016	0.257 ± 0.009	0.202 ± 0.004
Away from centre (In bridge)	0.27 ± 0.03	0.193 ± 0.010	0.183 ± 0.004

TABLE S7. Data for C10E4 (46.2 wt%) droplets in the same convention as Fig. S6.

$t(\tau)$	$t_c + [0, 12.5]$	$t_c + [13.75, 81.25]$	$t_c + [82.5, 360]$
$b(\sigma)$	$3.72 < b < 4.55$	$4.87 < b < 10.33$	$11.00 < b < 22.00$
Toward bridge (System)	0.2634 ± 0.0021	0.2684 ± 0.0016	0.2710 ± 0.0008
Away from bridge (System)	0.265 ± 0.004	0.2642 ± 0.0012	0.2593 ± 0.0008
Toward centre (In bridge)	0.445 ± 0.024	0.336 ± 0.010	0.277 ± 0.003
Away from centre (In bridge)	0.40 ± 0.05	0.325 ± 0.011	0.272 ± 0.003

TABLE S8. Data for Silwet-L77 droplets (51.2 wt%) in the same convention as Fig. S6.

$t(\tau)$	$t_c + [0, 12.5]$	$t_c + [13.75, 86.25]$	$t_c + [87.5, 598.75]$
$b(\sigma)$	$3.50 < b < 4.50$	$5.00 < b < 9.94$	$10.00 < b < 23.37$
Toward bridge (System)	0.2625 ± 0.0027	0.2703 ± 0.0014	0.2705 ± 0.0005
Away from bridge (System)	0.2685 ± 0.0030	0.2614 ± 0.0014	0.2616 ± 0.0005
Toward centre (In bridge)	0.45 ± 0.04	0.341 ± 0.010	0.2756 ± 0.0017
Away from centre (In bridge)	0.37 ± 0.03	0.334 ± 0.010	0.2699 ± 0.0027

VELOCITY OF APPROACH

In the main manuscript, the velocity of approach of C10E4 for different concentrations is reported, using the length of system in the X direction and its derivative with time. Here, we present the analogous data for C10E8 (Figure S7a) and Silwet-L77 (Figure S7b). The dynamics are similar to C10E4, as explained in the main manuscript. We also compare all three types of surfactants for the lowest (Figure S8a) and highest concentrations (Figure S8b). The data show that Silwet-L77 has the smallest maximum absolute velocity both in low and high concentrations. The surface tension of Silwet-L77 is around 20.7 mN/m [2], while the values for C10E4 and C10E8 are about 27 mN/m and 36 mN/m, respectively [3, 4].

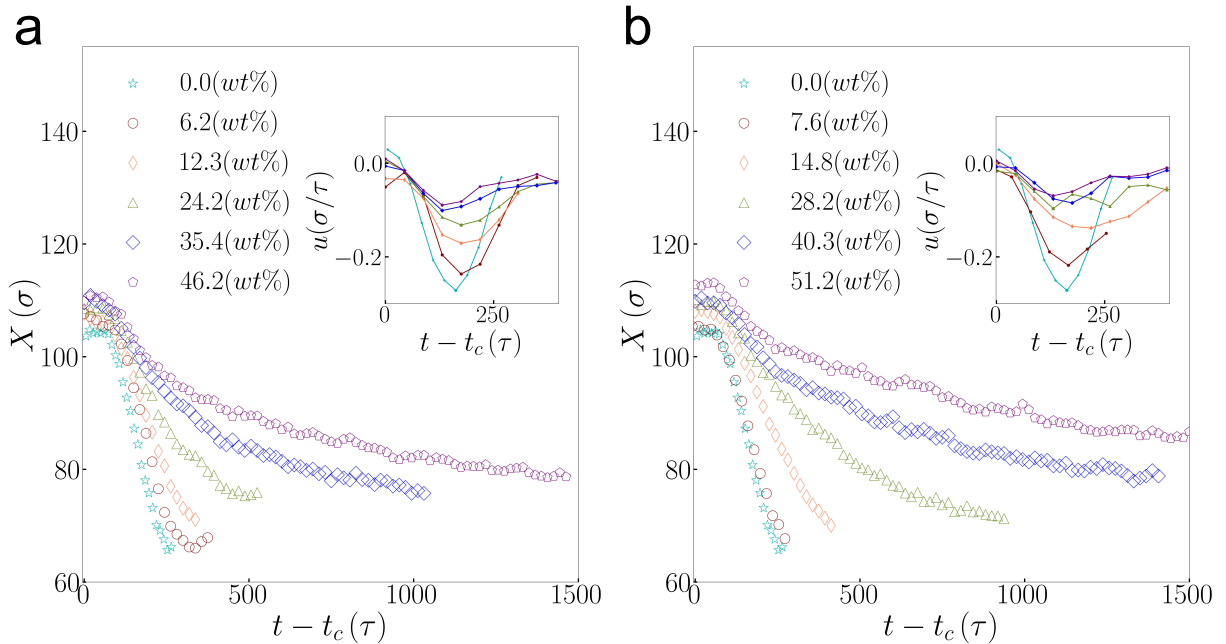


FIG. S7. System length X for droplets for different concentrations of a) C10E8 and b) Silwet-L77. Insets show the instantaneous velocity of approach $u = dX/dt$.

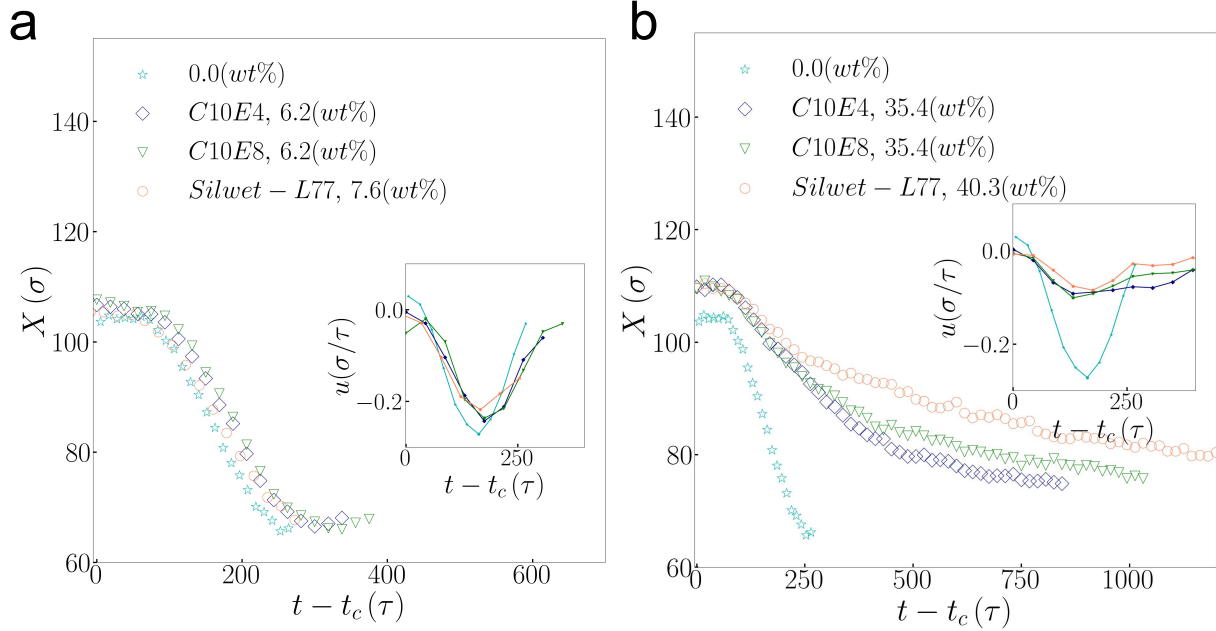


FIG. S8. comparison of velocity of approach in all three types of surfactants in a) low and b) high concentrations. When it comes to the maximum velocity, Silwet-L77 has the smallest.

ASPHERICITY OF THE DROPLETS

To characterise the structural features, we calculated the gyration tensor (Eq. 1) where N is the number of particles, x_i, y_i, z_i are coordinates of the particles and x_{cm}, y_{cm}, z_{cm} give the centre of mass of the system. Eigenvalues of the gyration tensor (Eq. 1) are found and sorted ($\lambda_1 \geq \lambda_2 \geq \lambda_3$) to obtain the gyration tensor trace (Eq. 2), and calculate asphericity (Eq. 3) — which is zero for a perfect spherical symmetry — for each snapshot. Figure S9 illustrates the asphericity of C10E4, C10E8, and Silwet-L77 laden droplets during the coalescence for different concentrations. Adding more surfactant causes significant changes in structural features. Higher concentration of surfactant leads to delayed creation of a single equilibrated sphere ($a_s = 0$). Moreover, comparison between all three types of surfactants in different concentrations are plotted in Figs S10a and b.

$$\frac{1}{N} \begin{pmatrix} \Sigma_i(x_i - x_{cm})^2 & \Sigma_i(x_i - x_{cm})\Sigma_i(y_i - y_{cm}) & \Sigma_i(x_i - x_{cm})\Sigma_i(z_i - z_{cm}) \\ \Sigma_i(x_i - x_{cm})\Sigma_i(y_i - y_{cm}) & \Sigma_i(y_i - y_{cm})^2 & \Sigma_i(y_i - y_{cm})\Sigma_i(z_i - z_{cm}) \\ \Sigma_i(x_i - x_{cm})\Sigma_i(z_i - z_{cm}) & \Sigma_i(y_i - y_{cm})\Sigma_i(z_i - z_{cm}) & \Sigma_i(z_i - z_{cm})^2 \end{pmatrix} \quad (1)$$

$$\text{Tr}S = \lambda_1 + \lambda_2 + \lambda_3 = R_g^2 \quad (2)$$

$$a_s = \lambda_1 - \frac{1}{2}(\lambda_2 + \lambda_3) \quad (3)$$

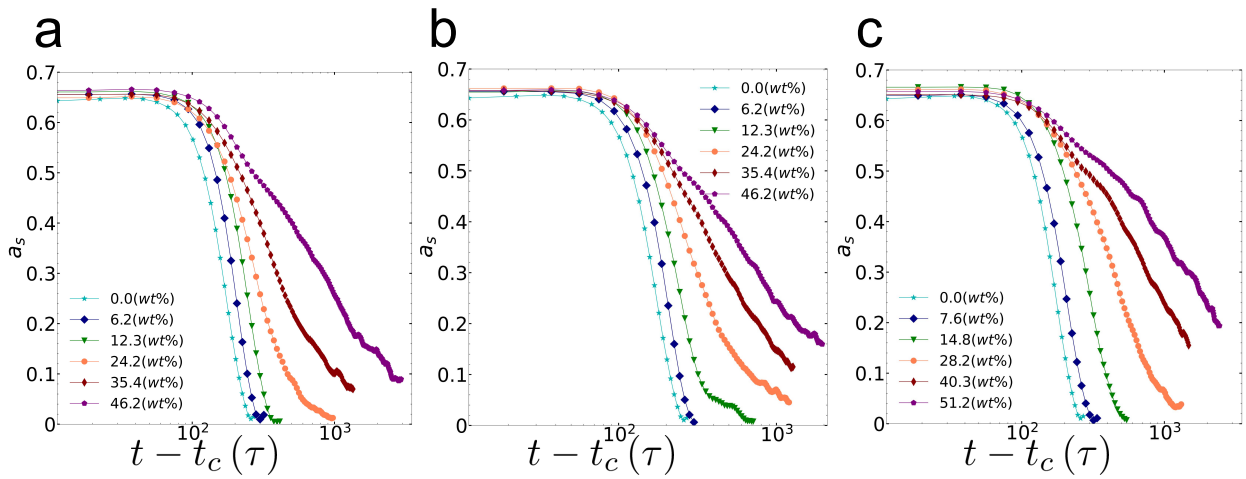


FIG. S9. Comparison of Asphericity (a_s) during the coalescence process of surfactant types a) C10E4, b) C10E8, and c) Silwet-L77.

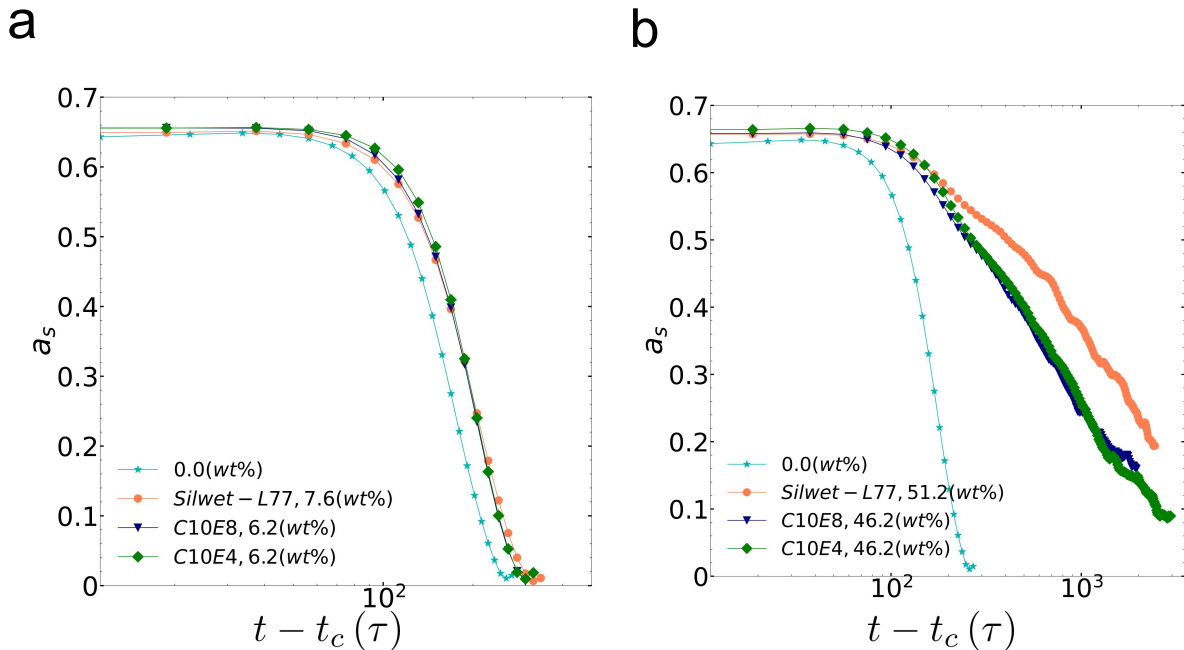


FIG. S10. comparison of Asphericity (a_s) in all three types of surfactants in a) low and b) high concentrations.

MOVIES

- File `M1_coalescence.mp4`: shows the coalescence of two surfactant-laden droplets (C10E4, 46.2 wt%)
- File `M2_pinching.mp4`: shows the pinching at the initial approach of the droplets (C10E4, 46.2 wt%)
- File `M3_bridge_zoom.mp4`: shows the bridge area of C10E4 (46.2 wt%, $t(\tau) = t_c + [0, 150]$) from the pinching point to a developed bridge. On the right, water beads and on the left surfactant beads during the coalescence are shown. It is evident that coalescence starts with surfactant beads (mainly the hydro phobic ones) and water joins much later.
- File `M4_mass_transport.mp4`: Here the inside of surfactant-laden droplets of C10E4 (46.2 wt%) are shown during the coalescence. The key points are surfactant movements inside the bridge (from bulk to surface) and the creation of new aggregates inside the bridge.

-
- [1] S. Perumanath, M. K. Borg, M. V. Chubynsky, J. E. Sprittles, and J. M. Reese, Phys. Rev. Lett. **122**, 104501 (2019).
 - [2] X. Tang, J. Dong, and X. Li, J. Colloid Interface Sci. **325**, 223 (2008).
 - [3] Y.-C. Lee, H.-S. Liu, S.-Y. Lin, H.-F. Huang, Y.-Y. Wang, and L.-W. Chou, J. Chin. Inst. Chem. Eng. **39**, 75 (2008).
 - [4] D. Anghel, S. Saito, A. Băran, A. Iovescu, and M. Cornițescu, Colloid Polym. Sci. **285**, 771 (2007).